

## Supporting Information

### **The Electrophilic Methylating Agent [SO<sub>2</sub>Me]<sup>+</sup> – Parent of Two Cationic Species**

Dirk Hollenwäger\*, Valentin Bockmair, and Andreas J. Kornath†

† passed away unexpectedly in march 2024

---

## Table of Contents

1	$^1\text{H}$ NMR spectroscopy .....	S3
1.1	$^1\text{H}$ NMR spectroscopy of $[\text{FS}(\text{OH})(\text{OMe})][\text{SbF}_6]$ .....	S3
1.2	$^1\text{H}$ NMR spectroscopy of $[\text{FS}(\text{OMe})_2][\text{Sb}_2\text{F}_{11}]$ .....	S4
2	Vibrational Data .....	S5
2.1	Vibrational Data of $[\text{FS}(\text{OMe})_2][\text{Sb}_2\text{F}_{11}]$ .....	S5
2.2	Vibrational Data of $[\text{FS}(\text{OH})(\text{OMe})][\text{SbF}_6]$ .....	S6
3	Crystallographic Data .....	S7
3.1	$[\text{FS}(\text{OMe})_2][\text{Sb}_2\text{F}_{11}]$ .....	S8
3.2	$[\text{FS}(\text{OH})(\text{OMe})][\text{SbF}_6]$ .....	S9
4	Quantum Chemical Calculations .....	S10
4.1	$[\text{FS}(\text{OH})(\text{OMe})]^+$ in the gas phase.....	S10
4.2	$[\text{FS}(\text{OH})(\text{OMe})]^+$ solvated with water.....	S12
4.3	Transition state of $[\text{FS}(\text{OH})(\text{OMe})]^+$ solvated with water .....	S13
4.4	Optimized structure of $[\text{S}(\text{O})(\text{OMe})]^+\cdot\text{HF}$ solvated with water .....	S15
4.5	$[\text{FS}(\text{OMe})_2]^+$ .....	S17
4.6	MEP calculations of $[\text{SO}_2\text{Me}]^+$ and $[\text{FS}(\text{OMe})_2]^+$ .....	S19
5	Experimental Section.....	S19
6	References .....	SFehler! Textmarke nicht definiert.

# 1 <sup>1</sup>H NMR spectroscopy

## 1.1 <sup>1</sup>H NMR spectroscopy of [FS(OH)(OMe)][SbF<sub>6</sub>]

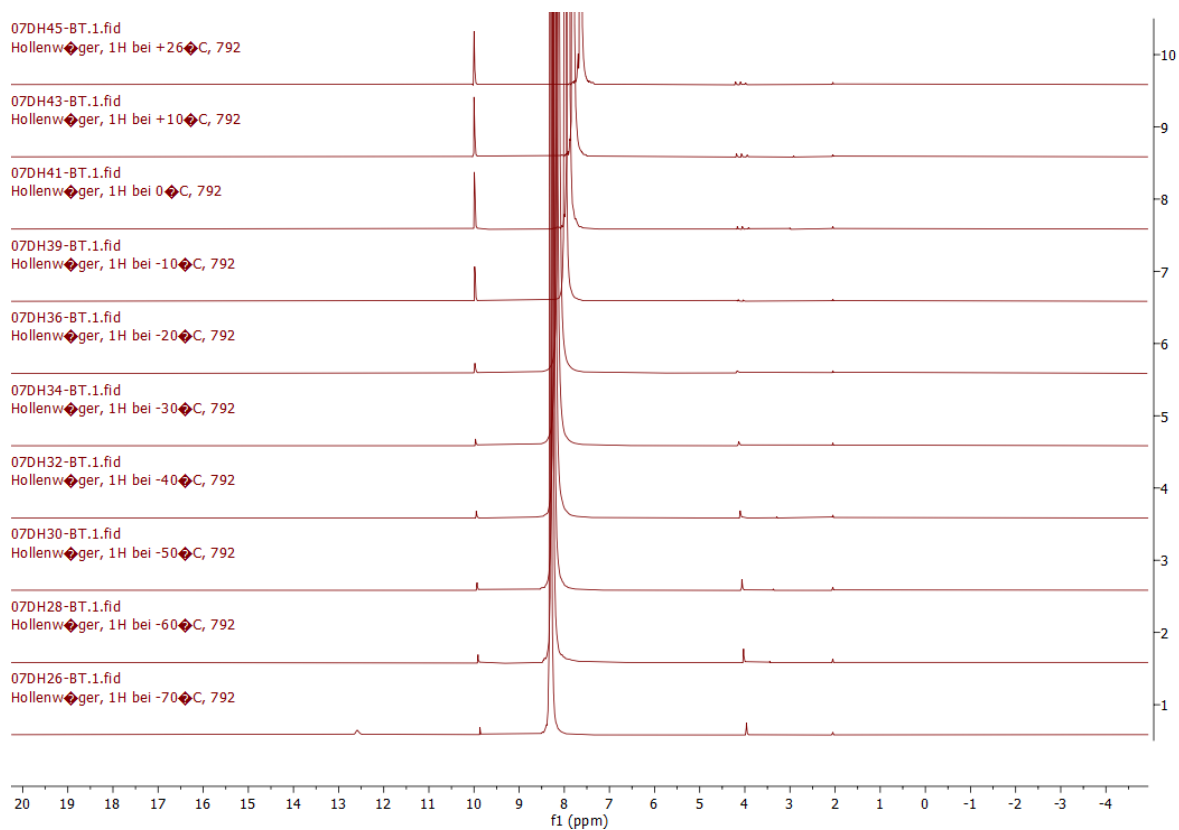


Figure S1. <sup>1</sup>H NMR spectra stack of [FS(OMe)<sub>2</sub>][Sb<sub>2</sub>F<sub>11</sub>] at various temperatures. The NMR spectra are measured with acetone-d<sub>6</sub> as external reference.

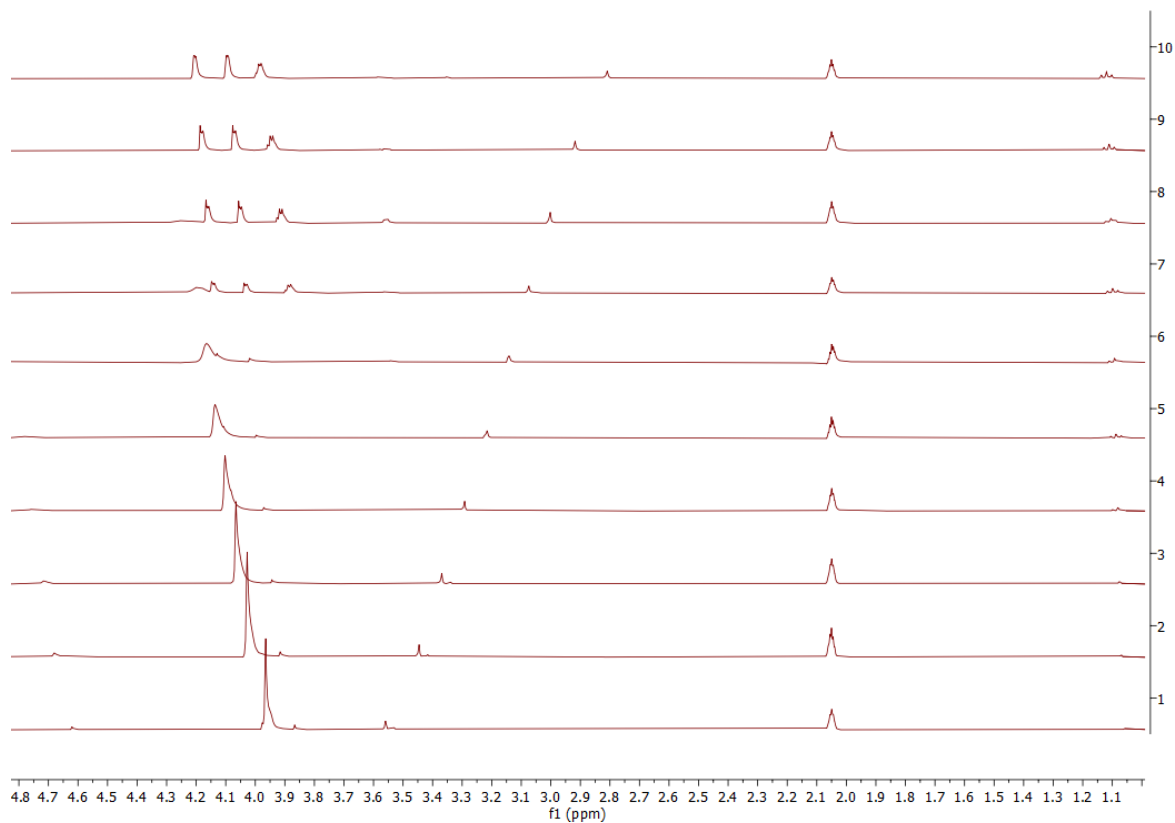


Figure S2. <sup>1</sup>H NMR spectra stack of [FS(OH)(OMe)][SbF<sub>6</sub>] at various temperatures from 1.00 ppm to 4.80 ppm. The NMR spectra are measured with acetone-d<sub>6</sub> as external reference.

## 1.2 $^1\text{H}$ NMR spectroscopy of $[\text{FS}(\text{OMe})_2][\text{Sb}_2\text{F}_{11}]$

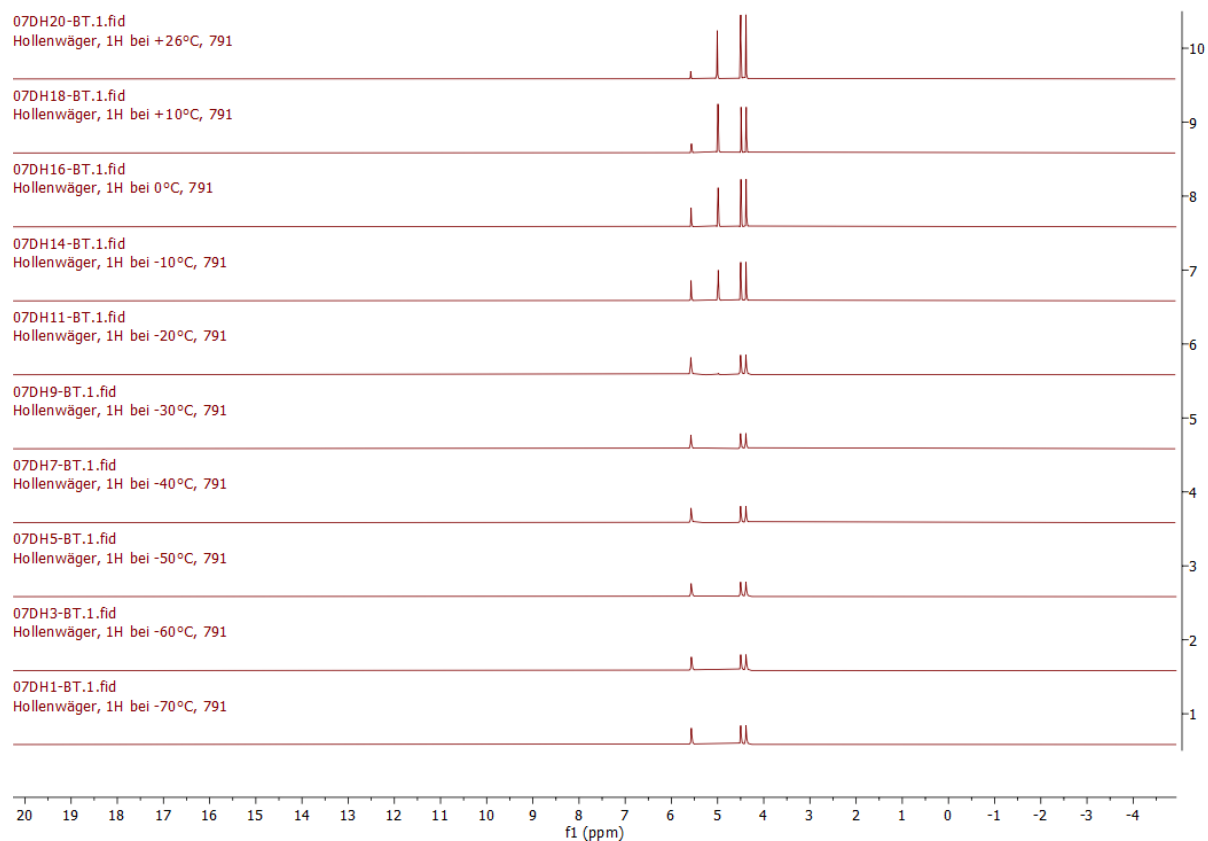


Figure S3.  $^1\text{H}$  NMR spectra stack of  $[\text{FS}(\text{OMe})_2][\text{Sb}_2\text{F}_{11}]$  at various temperatures. The NMR spectra are measured with acetone- $d_6$  as external reference.

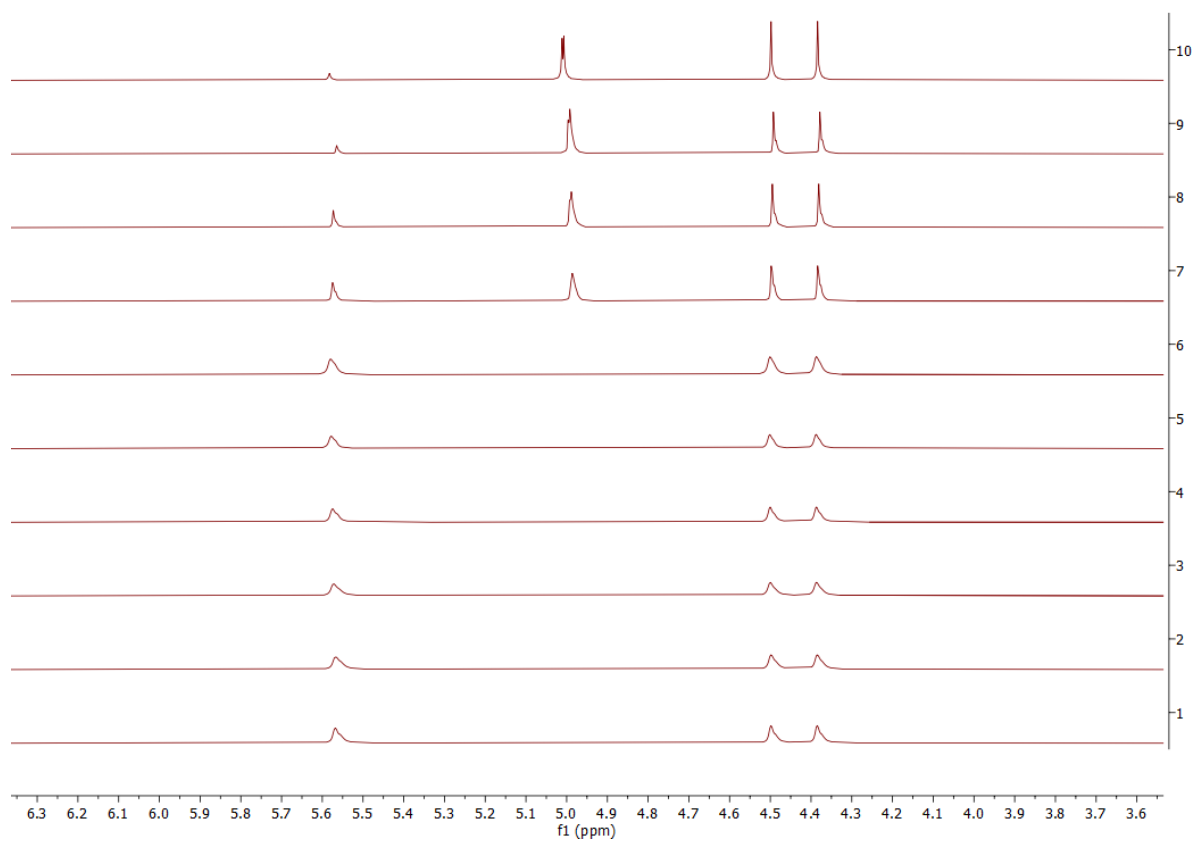


Figure S4.  $^1\text{H}$  NMR spectra stack of  $[\text{FS}(\text{OMe})_2][\text{Sb}_2\text{F}_{11}]$  at various temperatures from 3.55 ppm to 6.35 ppm. The NMR spectra are measured with acetone- $d_6$  as external reference.

## 2 Vibrational Data

### 2.1 Vibrational Data of [FS(OMe)<sub>2</sub>][Sb<sub>2</sub>F<sub>11</sub>]

Table S 1. Assignment of experimental vibrational frequencies [cm<sup>-1</sup>] of [FS(OMe)<sub>2</sub>][Sb<sub>2</sub>F<sub>11</sub>] and calculated vibrational frequencies [cm<sup>-1</sup>] of [FS(OMe)<sub>2</sub>]<sup>+</sup>.

[FS(OMe) <sub>2</sub> ][Sb <sub>2</sub> F <sub>11</sub> ] exp.		[FS(OMe) <sub>2</sub> ] <sup>+</sup> calc. <sup>[b,c]</sup>		
IR	Raman	IR/Raman	Assi	
3094(m)	3088(14)	3095(4/49)	V <sub>1</sub>	v <sub>as</sub> (CH)
		3087(4/45)	V <sub>2</sub>	v <sub>as</sub> (CH)
		3080(1/24)	V <sub>3</sub>	v <sub>as</sub> (CH)
		3057(0/30)	V <sub>4</sub>	v <sub>as</sub> (CH)
2987(m)	2994(65) 2855(15)	2975(1/119)	V <sub>5</sub>	v <sub>s</sub> (CH)
		2960(2/128)	V <sub>6</sub>	v <sub>s</sub> (CH)
1778(w)				
1445(s)	1447(20)	1440(17/5)	V <sub>7</sub>	δ(CH <sub>2</sub> )
		1432(20/4)	V <sub>8</sub>	δ(CH <sub>2</sub> )
		1424(16/5)	V <sub>9</sub>	δ(CH <sub>2</sub> )
		1422(17/3)	V <sub>10</sub>	δ(CH <sub>2</sub> )
		1417(0/1)	V <sub>11</sub>	γ(CH <sub>3</sub> )
		1411(3/1)	V <sub>12</sub>	γ(CH <sub>3</sub> )
1358(w)	1316(19)	1151(20/1)	V <sub>13</sub>	δ(CH <sub>3</sub> )
1300(w)	1171(14)	1139(8/2)	V <sub>14</sub>	δ(CH <sub>3</sub> )
		1125(1/1)	V <sub>15</sub>	δ(CH <sub>3</sub> )
1175(m)	1150(29)	1119(2/1)	V <sub>16</sub>	δ(CH <sub>3</sub> )
1022(vs)	1008(18)	1032(255/3)	V <sub>17</sub>	v(SO)
960(vs)	986(17) 955(15)	975(432/2)	V <sub>18</sub>	v(SO)
835(s)	838(27)	838(54/7)	V <sub>19</sub>	v(CO)
808(s)	813(20)	822(165/3)	V <sub>20</sub>	v(CF)
748(s)	757(58)	760(15/19)	V <sub>21</sub>	v(CO)
602(m)	604(14)			
555(s)	558(25) 412(18) 394(19) 363(14) 348(14)	538(13/3)	V <sub>22</sub>	δ(SO <sub>2</sub> )
		417(6/1)	V <sub>23</sub>	δ(SOF)
		377(22/1)	V <sub>24</sub>	δ(SOF)
		274(4/2)	V <sub>25</sub>	δ(SOC)
		180(13)	V <sub>26</sub>	δ(SOC)
		131(4/0)	V <sub>27</sub>	τ(CH <sub>3</sub> )
		107(3/0)	V <sub>28</sub>	τ(CH <sub>3</sub> )
	97(27)	85(5/0)	V <sub>29</sub>	τ(CH <sub>3</sub> )
		79(1/0)	V <sub>30</sub>	τ(CH <sub>3</sub> )
700(vs)	684(18)			
673(vs)	647(100)			
660(vs)	572(26)			
494(s)	280(46) 230(17)			

[a] Abbreviations for IR intensities: vs = very strong, s = strong, m = medium, w = weak, vw = very weak, sh = shoulder. Experimental Raman intensities are relative to a scale of 1 to 100. [b] Calculated on the M06-2X/aug-cc-pVTZ level of theory. Scaling factor 0.956. [c] IR intensities in km/mol; Raman intensities in Å<sup>4</sup>/u.

## 2.2 Vibrational Data of [FS(OH)(OMe)][SbF<sub>6</sub>]

Table S2. Experimental vibrational frequencies [cm<sup>-1</sup>] of [FS(OH)(OMe)][SbF<sub>6</sub>] and calculated vibrational frequencies [cm<sup>-1</sup>] of [FS(OH)(OMe)]<sup>+</sup>.

[FS(OH)(OMe)][SbF <sub>6</sub> ] (2) exp. <sup>[a]</sup>		[FS(OH)(OMe)] <sup>+</sup> calc. <sup>[b,c]</sup>	Assignment	
IR	Raman	IR/Raman		
3284(m)		3198(1598/133)	v <sub>1</sub>	v(OH)
3111(m)		3094(4/49)	v <sub>2</sub>	v <sub>as</sub> (CH)
	3085(26)	3078(1/22)	v <sub>3</sub>	v <sub>as</sub> (CH)
	2986(59)	2974(1/117)	v <sub>4</sub>	v <sub>as</sub> (CH)
1628(w)				
	1584(50)			
1445(vw)	1449(51)	1433(17/5)	v <sub>5</sub>	δ(CH <sub>2</sub> )
1418(vw)	1432(50)	1424(18/3)	v <sub>6</sub>	δ(CH <sub>2</sub> )
1373(vw)		1412(4/1)	v <sub>7</sub>	δ(CH <sub>2</sub> )
1319(vw)	1318(72)			
1292(vw)				
1234(vw)		1199(154/1)	v <sub>8</sub>	δ(SOH)
1209(vw)		1141(15/2)	v <sub>9</sub>	ρ(CH <sub>3</sub> )
1153(vw)	1171(45)	1121(1/1)	v <sub>10</sub>	ρ(CH <sub>3</sub> )
1020(w)	998(69)	1018(271/4)	v <sub>11</sub>	v(SO)
959(w)		947(168/7)	v <sub>12</sub>	v(SO)
879(vw)				
835(w)		841(187/4)	v <sub>13</sub>	v(SF)
808(w)	817(40)			
	732(51)	766(30/16)	v <sub>14</sub>	v(CO)
	689(71)			
586(w)	597(54)	588(55/1)	v <sub>15</sub>	δ(SOH)
555(w)		557(8/1)	v <sub>16</sub>	δ(SO <sub>2</sub> )
492(w)		401(43/1)	v <sub>17</sub>	δ(SO <sub>2</sub> )
		390(13/1)	v <sub>18</sub>	δ(SOF)
	134(42)	133(6/0)	v <sub>19</sub>	τ(CH <sub>3</sub> )
	97(51)	77(4/0)	v <sub>20</sub>	τ(CH <sub>3</sub> )
		26(0/0)	v <sub>21</sub>	δ(SOH)
Vibrations of anion SbF <sub>6</sub> <sup>-</sup>				
	680(81)			
658(vs)	653(100)			
	300(55)			
	230(56)			

[a] Abbreviations for IR intensities: vs = very strong, s = strong, m = medium, w = weak, sh = shoulder, br = broad. Experimental Raman intensities are relative to a scale of 1 to 100. [b] Calculated on the M06-2X/aug-cc-pVTZ level of theory. Scaling factor: 0.956. [c] IR intensities in km/mol; Raman intensities in Å<sup>4</sup>/u.

### 3 Crystallographic Data

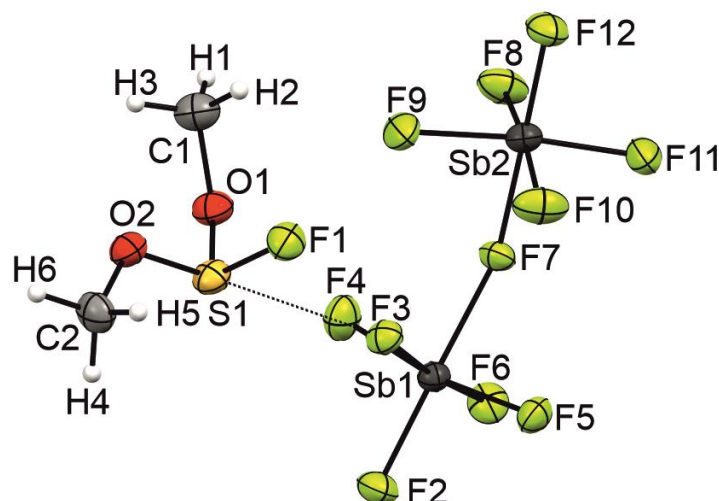
Table S3. Crystal data and structure refinement of [FS(OH)(OMe)][SbF<sub>6</sub>], [FS(OMe)<sub>2</sub>][Sb<sub>2</sub>F<sub>11</sub>]

	[FS(OH)(OMe)][SbF <sub>6</sub> ]	[FS(OMe) <sub>2</sub> ][Sb <sub>2</sub> F <sub>11</sub> ]
Molecular Formula	CH <sub>4</sub> F <sub>7</sub> O <sub>2</sub> SSb	C <sub>2</sub> H <sub>6</sub> F <sub>12</sub> O <sub>2</sub> SSb <sub>2</sub>
M <sub>r</sub> [g·mol <sup>-1</sup> ]	334.86	565.65
Crystal size [mm <sup>3</sup> ]	0.163x0.365x0.438	0.762x0.355x0.200
Crystal system	Orthorhombic	monoclinic
Space group	<i>Pca</i> 2 <sub>1</sub>	<i>P</i> 2 <sub>1</sub> / <i>n</i>
a [Å]	13.5681(5)	9.7473(9)
b [Å]	10.8817(5)	12.6004(9)
c [Å]	22.3347(8)	10.6035(8)
α [°]	90	90
β [°]	90	100.743
γ [°]	90	90
V [Å <sup>3</sup> ]	3297.6(2)	1279.50(18)
Z	16	4
ρ <sub>calc</sub> [g·cm <sup>-3</sup> ]	2.698	2.936
μ [mm <sup>-1</sup> ]	3.683	4.527
λ <sub>MoKα</sub> [Å]	0.71073	0.71073
F(000)	2496.0	1040.0
T [K]	102	103
h, k, l range	-10:17; -13:11; -28:26	-11:9; -14:13; -12:12
Measured reflexes	13848	8759
Unique reflexes	6546	2104
R <sub>int</sub>	0.0249	0.0540
Parameters	450	174
R(F)/wR(F <sup>2</sup> ) <sup>[a]</sup> (all data)	0.0279/0.0665	0.0483/ 0.0894
Weighting scheme <sup>[b]</sup>	0.018600/5.787000	0.045400/0.894200
S (GoF) <sup>[c]</sup>	1.102	1.079
Residual density [e·Å <sup>-3</sup> ]	0.988/-0.959	1.256/-0.700
Device	Oxford XCalibur	Oxford XCalibur
CCDC	2368718	2368721

[a]  $R_1 = \sum ||F_o| - |F_c|| / \sum |F_o|$ .

[b]  $wR_2 = [\sum [w(F_o^2 - F_c^2)^2] / \sum [w(F_o^2)]]^{1/2}$ ;  $w = [\sigma_c^2(F_o^2) + (xP)^2 + yP]^{-1}$ ;  $P = (F_o^2 + 2F_c^2) / 3$ .

[c]  $GoF = \{\sum [w(F_o^2 - F_c^2)^2] / (n-p)\}^{1/2}$  (n = number of reflections; p = total number of parameters).

Figure S5. asymmetric unit of [FS(OMe)<sub>2</sub>][Sb<sub>2</sub>F<sub>11</sub>] (displacement ellipsoids 50% probability).Table S4. Bond lengths, angles, torsions angles and donor-acceptor interactions of the asymmetric unit of [FS(OMe)<sub>2</sub>][Sb<sub>2</sub>F<sub>11</sub>], *i*=1-x,1-y,1-z, *ii*= -1/2+x,1.5-y,-1/2+z, *iii*= 1/2-x,1/2+y,1/2-z, *iv*= -1/2+x,1.5-y,1/2+z

Bond lengths [Å]		Bond angles [°]		Torsions angles [°]		Donor-acceptor interactions [Å]	
S1-O1	1.517(6)	O1-S1-O2	102.3(3)	O2-S1-O1-C1	44.7(7)	S1-F2 <i>i</i>	2.996(5)
S1-O2	1.535(5)	O1-S1-F1	102.5(3)	F1-S1-O1-C1	-58.3(6)	C1(-H2) ⋯F10 <i>ii</i>	2.970(9)
S1-F1	1.558(5)	O2-S1-F1	99.7(3)	O1-S1-O2-C2	169.3(5)	C2(-H6) ⋯F4 <i>iii</i>	3.227(10)
O1-C1	1.476(9)	C1-O1-S1	122.0(5)	F1-S1-O2-C2	-85.6(6)	S1-F3	2.910(4)
O2-C2	1.488(9)	C2-O2-S1	117.5(4)			S1-F12 <i>iv</i>	3.066(5)
Sb1-F2	1.855(4)	F4-Sb1-F6	90.3(2)				
Sb1-F3	1.863(4)	F4-Sb1-F2	96.2(2)				
Sb1-F4	1.849(4)	F6-Sb1-F2	92.8(2)				
Sb1-F5	1.857(4)	F4-Sb1-F5	169.6(2)				
Sb1-F6	1.854(4)	F6-Sb1-F5	91.20(19)				
Sb1-F7	2.031(4)	F2-Sb1-F5	94.0(2)				
Sb2-F7	2.028(4)	F3-Sb1-F3	88.44(19)				
Sb2-F8	1.852(4)	F6-Sb1-F3	173.66(19)				
Sb2-F9	1.858(4)	F2-Sb1-F3	93.5(2)				
Sb2-F10	1.843(4)	F5-Sb1-F3	88.95(18)				
Sb2-F11	1.861(4)	F4-Sb1-F7	84.37(19)				
Sb2-F12	1.860(4)	F6-Sb1-F7	86.40(18)				
		F2-Sb1-F7	179.03(18)				
		F5-Sb1-F7	85.47(18)				
		F3-Sb1-F7	87.29(17)				
		Sb2-F7-Sb1	146.4(2)				
		F10-Sb2-F8	170.9(2)				
		F10-Sb2-F9	91.0(2)				
		F10-Sb2-F11	89.5(2)				
		F10-Sb2-F7	85.75(19)				
		F12-Sb2-F11	93.6(2)				
		F12-Sb2-F7	179.25(18)				
		F11-Sb2-F7	87.11(18)				



F8-Sb2-F9	88.1(2)
F8-Sb2-F12	95.1(2)
F9-Sb2-F12	93.3(2)
F8-Sb2-F11	90.4(2)
F9-Sb2-F11	173.1(2)
F8-Sb2-F7	85.19(19)
F9-Sb2-F7	86.04(18)

### 3.2 [FS(OH)(OMe)][SbF<sub>6</sub>]

Table S5. Bond lengths, angles, torsions angles and donor-acceptor interactions within the asymmetric unit of [FS(OH)(OMe)][SbF<sub>6</sub>]

Bond lengths [Å]							
S1-O1	1.532(6)	Sb1-F5	1.865(5)	Sb3-F21	1.864(5)		
S1-O2	1.507(6)	Sb1-F6	1.870(5)	Sb3-F22	1.871(5)		
S1-F1	1.549(5)	Sb1-F7	1.914(5)	Sb4-F23	1.903(5)		
O2-C1	1.486(11)	Sb1-F8	1.873(5)	Sb4-F24	1.873(5)		
S2-O3	1.528(7)	Sb1-F9	1.869(5)	Sb4-F25	1.871(5)		
S2-O4	1.526(7)	Sb1-F10	1.861(5)	Sb4-F26	1.864(5)		
S2-F2	1.561(6)	Sb2-F11	1.867(5)	Sb4-F27	1.855(5)		
O4-C2	1.486(11)	Sb2-F12	1.863(5)	Sb4-F28	1.874(5)		
S3-O5	1.521(7)	Sb2-F13	1.859(5)				
S3-O6	1.515(6)	Sb2-F14	1.863(5)				
S3-F3	1.556(6)	Sb2-F15	1.909(5)				
O6-C3	1.484(12)	Sb2-F16	1.868(5)				
S4-O7	1.522(7)	Sb3-F17	1.874(5)				
S4-O8	1.517(6)	Sb3-F18	1.875(5)				
S4-F4	1.559(6)	Sb3-F19	1.912(5)				
O8-C4	1.496(11)	Sb3-F20	1.863(5)				
Bond angles [°]							
O2-S1-O1	104.7(4)	F10-Sb1-F6	92.1(2)	F14-Sb2-F16	90.0(3)	F21-Sb3-F19	89.3(3)
O1-S1-F1	97.5(4)	F5-Sb1-F6	91.4(2)	F12-Sb2-F16	91.8(2)	F22-Sb3-F19	179.2(3)
O2-S1-F1	100.8(3)	F9-Sb1-F6	90.9(2)	F11-Sb2-F16	178.0(3)	F17-Sb3-F19	88.9(2)
C1-O2-S1	123.8(6)	F10-Sb1-F8	89.8(2)	F13-Sb2-F15	89.7(2)	F18-Sb3-F19	88.7(2)
O4-S2-O3	104.1(4)	F5-Sb1-F8	177.7(2)	F14-Sb2-F15	88.6(2)	F27-Sb4-F26	90.3(3)
O3-S2-F2	97.4(4)	F9-Sb1-F8	89.7(2)	F12-Sb2-F15	178.0(2)	F27-Sb4-F25	90.2(3)
O4-S2-F2	101.1(4)	F6-Sb1-F8	90.8(2)	F11-Sb2-F15	88.2(2)	F26-Sb4-F25	178.1(2)
C2-O4-S2	123.7(6)	F10-Sb1-F7	88.8(2)	F16-Sb2-F15	89.9(3)	F27-Sb4-F24	178.0(3)
O6-S3-O5	104.6(4)	F5-Sb1-F7	90.2(2)	F20-Sb3-F21	90.9(2)	F26-Sb4-F24	90.6(3)
O5-S3-F3	97.5(4)	F9-Sb1-F7	88.2(2)	F20-Sb3-F22	91.0(2)	F25-Sb4-F24	88.9(3)
O6-S3-F3	101.0(3)	F6-Sb1-F7	178.1(3)	F21-Sb3-F22	91.5(2)	F27-Sb4-F28	91.8(3)
C3-O6-S3	123.0(6)	F8-Sb1-F7	87.5(2)	F20-Sb3-F17	178.1(2)	F26-Sb4-F28	91.3(2)
O8-S4-O4	100.6(3)	F13-Sb2-F14	178.3(2)	F21-Sb3-F17	89.9(2)	F25-Sb4-F28	90.5(2)
O7-S4-F4	96.5(4)	F13-Sb2-F12	91.3(2)	F22-Sb3-F17	90.7(2)	F24-Sb4-F28	90.0(3)
O8-S4-F4	104.7(4)	F14-Sb2-F12	90.4(2)	F20-Sb3-F18	89.7(2)	F27-Sb4-F23	88.5(3)
C4-O8-S4	122.6(6)	F13-Sb2-F11	90.6(2)	F21-Sb3-F18	177.9(2)	F26-Sb4-F23	89.0(2)
F10-Sb1-F5	90.6(2)	F14-Sb2-F11	89.2(3)	F22-Sb3-F18	90.5(2)	F25-Sb4-F23	89.2(2)
F10-Sb1-F9	177.0(2)	F12-Sb2-F11	90.1(2)	F17-Sb3-F18	89.4(2)	F24-Sb4-F3	89.6(2)
F5-Sb1-F9	89.8(2)	F13-Sb2-F16	90.1(3)	F20-Sb3-F19	89.4(2)	F28-Sb4-F23	179.5(3)
Torsion Angles [°]							

O1-S1-O2-C1	-37.1(8)	O3-S2-O4-C2	34.9(8)	O5-S3-O6-C3	41.5(8)	O7-S4-O8-C4	-37.6(8)
F1-S1-O2-C1	63.7(7)	F2-S2-O4-C2	-65.7(8)	F3-S3-O6-C3	-59.4(8)	F4-S4-O8-C4	62.1(7)
Donor-acceptor interactions [Å]							
O1(-H1)···F23	2.544(9)	S1-F6	2.751(5)	O1-F6	2.913(8)		
C4(-H14)···F10	3.491(10)	S1-F14	2.743(6)	O1-F14	2.981(8)		

## 4 Quantum Chemical Calculations

The optimized structures are given with their cartesian coordinates x, y, z in angstrom. An illustration of the respective structures together with the calculated bond lengths in angstrom is shown next to the tables. The structures were calculated on the M062x/aug-cc-pVTZ level of theory.

### 4.1 [FS(OH)(OMe)]<sup>+</sup> in the gas phase

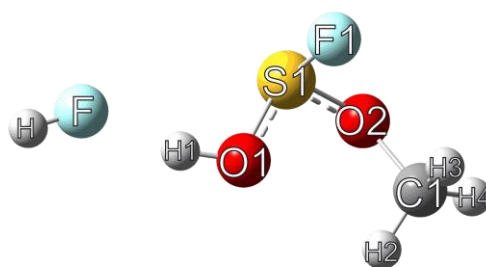


Figure S6. Optimized gas phase structure of [FS(OH)(OMe)]<sup>+</sup> on the M062x/aug-cc-pVTZ level of theory.

Table S6. Input matrix for the structure optimization of [FS(OH)(OMe)]<sup>+</sup> on the M062x/aug-cc-pVTZ level of theory.

# opt freq=raman M062x/aug-cc-pvtz geom=connectivity

Symbolic Z-matrix:

Charge = +1	Multiplicity = 1		
F	-3.115486	-0.315383	-0.040868
S	0.104833	0.370304	-0.481729
F	0.412262	1.485862	0.567334
O	1.481787	-0.237856	-0.692400
O	-0.581970	-0.654156	0.455693
C	2.271726	-0.856057	0.401408
H	2.349272	-0.144198	1.217116
H	3.232648	-1.042792	-0.060930
H	1.776433	-1.774554	0.695421
H	-1.571593	-0.639329	0.379593
H	-3.963954	-0.585875	0.223492

Calculation Type = FREQ

Calculation Method = RM062X

Basis Set = Aug-CC-pVTZ

Charge = 1

Spin = Singlet

Solvation = None

---

E(RM062X) = -789.14754 Hartree

RMS Gradient Norm = 9.908e-06 Hartree/Bohr

Imaginary Freq = 0

Dipole Moment = 2.5311744 Debye

Polarizability (?) = 43.715 a.u.

Point Group = C1

Job cpu time: 0 days 5 hours 11 minutes 5.9 seconds.

Thermo Tab Data Section:

Imaginary Freq = 0

Temperature = 298.15 Kelvin

Pressure = 1 atm

Frequencies scaled by = 1

Electronic Energy (EE) = -789.14754 Hartree

Zero-point Energy Correction = 0.072817 Hartree

Thermal Correction to Energy = 0.082168 Hartree

Thermal Correction to Enthalpy = 0.083112 Hartree

Thermal Correction to Free Energy = 0.036427 Hartree

EE + Zero-point Energy = -789.07473 Hartree

EE + Thermal Energy Correction = -789.06538 Hartree

EE + Thermal Enthalpy Correction = -789.06443 Hartree

EE + Thermal Free Energy Correction = -789.11112 Hartree

E (Thermal) = 51.561 kcal/mol

Heat Capacity (Cv) = 28.614 cal/mol-kelvin

Entropy (S) = 98.258 cal/mol-kelvin

Opt Tab Data Section:

Step number = 1

Maximum force = 0 Converged

RMS force = 0 Converged

Maximum displacement = 4.9e-05 Converged

RMS displacement = 2.2e-05 Converged

Predicted energy change = -3.272345e-12 Hartree

## 4.2 [FS(OH)(OMe)]<sup>+</sup> solvated with water

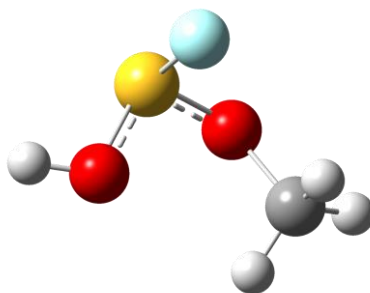


Figure S7. Optimized water solvated structure of [FS(OH)(OMe)]<sup>+</sup> on the M062x/aug-cc-pVTZ level of theory.

Table S7. Input matrix for the structure optimization of [FS(OH)(OMe)]<sup>+</sup> on the M062x/aug-cc-pVTZ level of theory.

# opt=(calcall,tight) freq=raman aug-cc-pvtz scrf=(solvent=water) geom=connectivity m062x

Symbolic Z-matrix:

Charge = +1	Multiplicity = 1		
S	0.846738	-1.143627	0.592160
F	-0.899997	-0.148551	-0.689000
O	0.724717	1.203817	0.428791
O	-1.866871	0.082318	0.407447
C	-1.614637	-0.572572	1.234184
H	-2.816612	-0.181786	-0.037265
H	-1.824082	1.130058	0.679375
H	1.568547	1.680415	0.317031
H	0.846738	-1.143627	0.592160

Calculation Type = FREQ

Calculation Method = RM062X

Basis Set = Aug-CC-pVTZ

Charge = 1

Spin = Singlet

Solvation = scrf=solvent=water

E(RM062X) = -688.7646 Hartree

RMS Gradient Norm = 2.5313e-05 Hartree/Bohr

Imaginary Freq = 0

Dipole Moment = 2.7667907 Debye

Polarizability (?) = 46.511 a.u.

Point Group = C1

Job cpu time: 0 days 1 hours 22 minutes 10.6 seconds.

Thermo Tab Data Section:

Imaginary Freq = 0

Temperature = 298.15 Kelvin

Pressure = 1 atm

Frequencies scaled by = 1

Electronic Energy (EE) = -688.7646 Hartree

Zero-point Energy Correction = 0.061462 Hartree

Thermal Correction to Energy = 0.067831 Hartree

Thermal Correction to Enthalpy = 0.068776 Hartree

Thermal Correction to Free Energy = 0.03093 Hartree

EE + Zero-point Energy = -688.70314 Hartree

EE + Thermal Energy Correction = -688.69677 Hartree

EE + Thermal Enthalpy Correction = -688.69583 Hartree

EE + Thermal Free Energy Correction = -688.73367 Hartree

E (Thermal) = 42.565 kcal/mol

Heat Capacity (Cv) = 20.252 cal/mol-kelvin

Entropy (S) = 79.653 cal/mol-kelvin

Opt Tab Data Section:

Step number = 1

Maximum force = 0 Converged

RMS force = 0 Converged

Maximum displacement = 4.4e-05 Converged

RMS displacement = 2e-05 Converged

Predicted energy change = -1.734397e-12 Hartree

### 4.3 Transition state of [FS(OH)(OMe)]<sup>+</sup> solvated with water

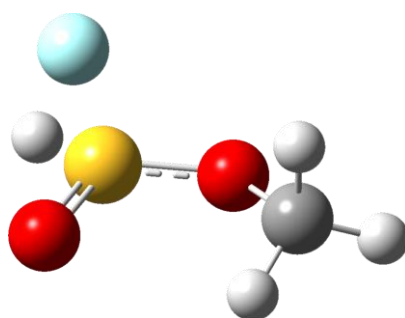


Figure S8. Optimized water solvated structure of the Transition state of [FS(OH)(OMe)]<sup>+</sup> on the M062x/aug-cc-pVTZ level of theory.

Table S8. Input matrix for the structure optimization of [FS(OH)(OMe)]<sup>+</sup> on the M062x/aug-cc-pVTZ level of theory.

# opt freq aug-cc-pvtz scrf=(solvent=water) geom=connectivity m062x

Symbolic Z-matrix:

Charge = +1	Multiplicity = 1		
S	-0.468248	-0.488616	-0.459645
F	-1.176815	1.169102	-0.079717

---

O	0.986717	-0.148863	-0.642975
O	-0.782049	-0.677763	0.984327
C	1.896038	0.340761	0.423528
H	1.673194	1.392852	0.563424
H	2.880765	0.181704	0.006586
H	1.722406	-0.247325	1.316662
H	-1.206640	0.537152	0.913120

---

Calculation Type = FREQ

Calculation Method = RM062X

Basis Set = Aug-CC-pVTZ

Charge = 1

Spin = Singlet

Solvation = scrf=solvent=water

E(RM062X) = -688.69477 Hartree

RMS Gradient Norm = 2.6933e-05 Hartree/Bohr

Imaginary Freq = 1

Dipole Moment = 1.6485653 Debye

Polarizability (?) = 48.871 a.u.

Point Group = C1

Job cpu time: 0 days 1 hours 2 minutes 0.3 seconds.

Thermo Tab Data Section:

Imaginary Freq = 1

Temperature = 298.15 Kelvin

Pressure = 1 atm

Frequencies scaled by = 1

Electronic Energy (EE) = -688.69477 Hartree

Zero-point Energy Correction = 0.056725 Hartree

Thermal Correction to Energy = 0.062587 Hartree

Thermal Correction to Enthalpy = 0.063531 Hartree

Thermal Correction to Free Energy = 0.026975 Hartree

EE + Zero-point Energy = -688.63804 Hartree

EE + Thermal Energy Correction = -688.63218 Hartree

EE + Thermal Enthalpy Correction = -688.63124 Hartree

EE + Thermal Free Energy Correction = -688.66779 Hartree

E (Thermal) = 39.274 kcal/mol

Heat Capacity (Cv) = 18.746 cal/mol-kelvin

Entropy (S) = 76.939 cal/mol-kelvin

Opt Tab Data Section:

Step number = 1

Maximum force = 7e-06 Converged

RMS force = 3e-06 Converged

Maximum displacement = 0.000409 Converged

RMS displacement = 0.000203 Converged

Predicted energy change = -9.781114e-10 Hartree

#### 4.4 Optimized structure of [S(O)(OMe)]<sup>+</sup>-HF solvated with water

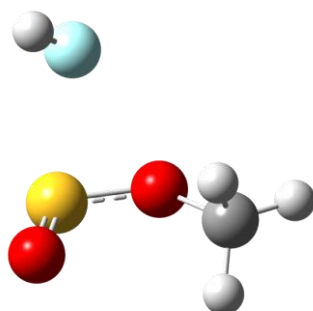


Figure S9. Optimized water solvated structure of the Transition state of [FS(OH)(OMe)]<sup>+</sup> on the M062x/aug-cc-pVTZ level of theory.

Table S9. Input matrix for the structure optimization of [FS(OH)(OMe)]<sup>+</sup> on the M062x/aug-cc-pVTZ level of theory.

# opt freq aug-cc-pvtz scrf=(solvent=water) geom=connectivity m062x

Symbolic Z-matrix:

Charge = +1	Multiplicity = 1		
S	-0.146813	-0.794632	-0.449079
F	-1.752499	1.118497	0.058408
O	0.823518	0.342780	-0.672934
O	-0.126838	-1.274783	0.884385
C	1.615958	0.962470	0.411432
H	0.913043	1.385800	1.122256
H	2.200145	1.719029	-0.093263
H	2.231962	0.189436	0.858017
H	-2.492824	1.034575	0.612376

Calculation Type = FREQ

Calculation Method = RM062X

Basis Set = Aug-CC-pVTZ

Charge = 1

Spin = Singlet

Solvation = scrf=solvent=water

E(RM062X) = -688.75103 Hartree

RMS Gradient Norm = 1.2761e-05 Hartree/Bohr

---

Imaginary Freq = 0

Dipole Moment = 0.26565543 Debye

Polarizability (?) = 48.533 a.u.

Point Group = C1

Job cpu time: 0 days 1 hours 5 minutes 14.3 seconds.

Thermo Tab Data Section:

Imaginary Freq = 0

Temperature = 298.15 Kelvin

Pressure = 1 atm

Frequencies scaled by = 1

Electronic Energy (EE) = -688.75103 Hartree

Zero-point Energy Correction = 0.058636 Hartree

Thermal Correction to Energy = 0.066588 Hartree

Thermal Correction to Enthalpy = 0.067533 Hartree

Thermal Correction to Free Energy = 0.025208 Hartree

EE + Zero-point Energy = -688.69239 Hartree

EE + Thermal Energy Correction = -688.68444 Hartree

EE + Thermal Enthalpy Correction = -688.6835 Hartree

EE + Thermal Free Energy Correction = -688.72582 Hartree

E (Thermal) = 41.785 kcal/mol

Heat Capacity (Cv) = 23.433 cal/mol-kelvin

Entropy (S) = 89.08 cal/mol-kelvin

Opt Tab Data Section:

Step number = 1

Maximum force = 1.8e-05 Converged

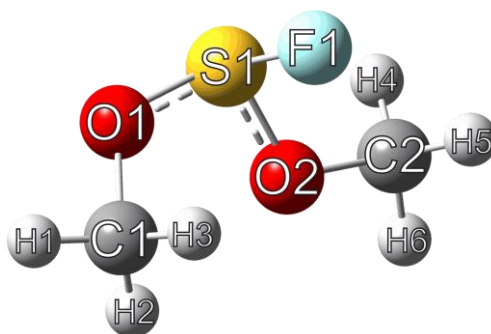
RMS force = 8e-06 Converged

Maximum displacement = 0.001038 Converged

RMS displacement = 0.000459 Converged

Predicted energy change = -6.241065e-09 Hartree



Figure S10. Optimized gas phase structure of [FS(OMe)<sub>2</sub>]<sup>+</sup> on the M062x/aug-cc-pVTZ level of theory.Table S 10. Input matrix for the structure optimization of [FS(OMe)<sub>2</sub>]<sup>+</sup> on the M062x/aug-cc-pVTZ level of theory.

# opt freq=raman M062x/aug-cc-pvtz geom=connectivity

Symbolic Z-matrix:

Charge = +1	Multiplicity = 1		
S	0.048359	0.467458	-0.544311
F	0.001917	1.393761	0.721092
O	0.838993	-0.723707	0.045097
O	-1.367648	-0.077165	-0.598728
C	2.307947	-0.593352	0.158887
H	2.707570	-0.191814	-0.769315
H	2.649102	-1.607887	0.322247
H	2.526306	0.043408	1.010273
C	-1.983657	-0.867769	0.497273
H	-1.512593	-1.843783	0.510533
H	-1.852325	-0.327300	1.429360
H	-3.025559	-0.922101	0.208133

Calculation Type = FREQ

Calculation Method = RM062X

Basis Set = Aug-CC-pVTZ

Charge = 1

Spin = Singlet

Solvation = None

E(RM062X) = -727.97532 Hartree

RMS Gradient Norm = 3.244e-06 Hartree/Bohr

Imaginary Freq = 0

Dipole Moment = 1.7591638 Debye

Polarizability (?) = 49.984667 a.u.

Point Group = C1

Job cpu time: 0 days 5 hours 14 minutes 57.4 seconds.

Thermo Tab Data Section:

---

Imaginary Freq = 0

Temperature = 298.15 Kelvin

Pressure = 1 atm

Frequencies scaled by = 1

Electronic Energy (EE) = -727.97532 Hartree

Zero-point Energy Correction = 0.090431 Hartree

Thermal Correction to Energy = 0.098321 Hartree

Thermal Correction to Enthalpy = 0.099265 Hartree

Thermal Correction to Free Energy = 0.057546 Hartree

EE + Zero-point Energy = -727.88489 Hartree

EE + Thermal Energy Correction = -727.877 Hartree

EE + Thermal Enthalpy Correction = -727.87606 Hartree

EE + Thermal Free Energy Correction = -727.91778 Hartree

E (Thermal) = 61.697 kcal/mol

Heat Capacity (Cv) = 25.003 cal/mol-kelvin

Entropy (S) = 87.805 cal/mol-kelvin

Opt Tab Data Section:

Step number = 1

Maximum force = 0 Converged

RMS force = 0 Converged

Maximum displacement = 0.000126 Not converged

RMS displacement = 4.1e-05 Not converged

Predicted energy change = -1.219271e-11 Hartree

#### 4.6 MEP calculations of $[\text{SO}_2\text{Me}]^+$ and $[\text{FS}(\text{OMe})_2]^+$

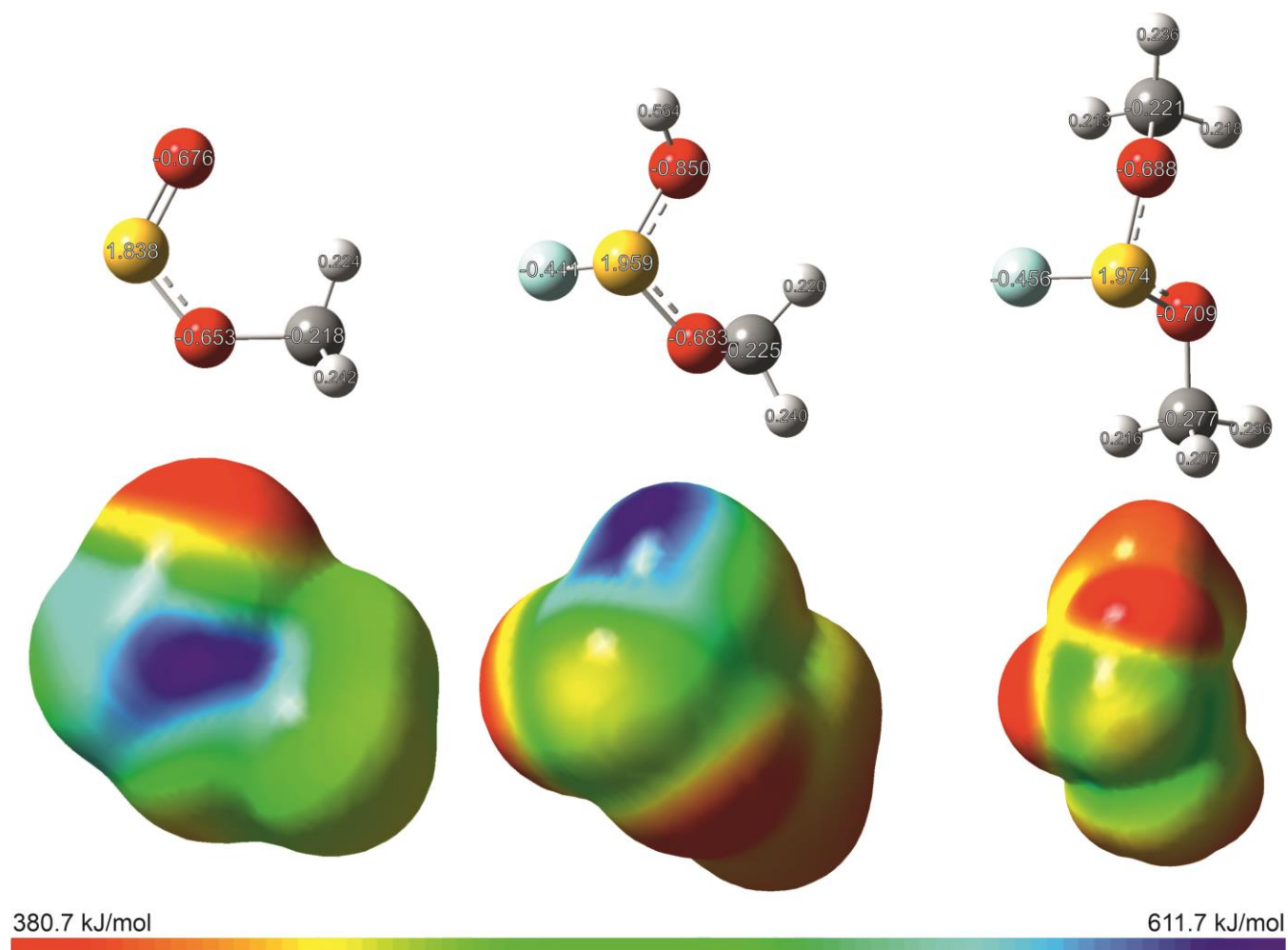


Figure S11. Molecular  $0.0004 \text{ bohr}^{-3}$  3D isosurfaces with mapped electrostatic potential as color scale from 380.7 kJ/mol (red) to 611.7 kJ/mol (blue). The electrostatic potential isosurfaces and the NPA charges have been calculated for  $[\text{SO}_2\text{Me}]^+$ ,  $[\text{FS}(\text{OH})(\text{OMe})]^+$  and  $[\text{FS}(\text{OMe})_2]^+$ .

## 5 Experimental Section

### General

Caution! The hydrolysis of  $\text{SbF}_5$  and the prepared salts  $[\text{SO}_2\text{Me}][\text{SbF}_6]$ ,  $[\text{FS}(\text{OH})(\text{OMe})][\text{SbF}_6]$  and  $[\text{FS}(\text{OMe})_2][\text{Sb}_2\text{F}_{11}]$  might form HF which burns skin and causes irreparable damage. Safety precautions must be taken while using and handling these materials.

### Apparatus and Materials

**Apparatus and Materials:** All reactions were carried out using standard Schlenk techniques on a stainless-steel vacuum line. The salt syntheses were carried out in FEP/PFA reactors with stainless steel valves. Before each reaction or NMR measurement, the stainless-steel vacuum line and the reactors were dried with fluorine. A Bruker MultiRam FT-Raman spectrometer with Nd: YAG laser excitation ( $\lambda = 1064 \text{ nm}$ ) was used for Raman measurements. The measurement was performed after the transfer of the sample into a cooled ( $-196^\circ\text{C}$ ) glass cell under a nitrogen atmosphere and subsequent evacuation of the glass cell. Low-temperature IR spectroscopy was carried out on a Bruker Vertex-80V FTIR spectrometer using a cooled cell with a single crystal CsBr plate on which small amounts of the samples were placed.<sup>1</sup> Single crystal X-ray diffraction studies were performed on an Oxford XCalibur3 diffractometer equipped with a Spellman generator (voltage 50 kV, current 40 mA) and a KappaCCD detector operating with Mo-K $\alpha$  radiation ( $\lambda = 0.7107 \text{ \AA}$ ). Measurements were performed at 173 K. The CrysAlisPro 1.171.39.46e program (Rigaku Oxford Diffraction, 2018) was used for data acquisition and reduction.<sup>2</sup> The structures were solved utilizing SHELXT<sup>3</sup> and SHELXL-2018/3<sup>4</sup> of the WINGX software package.<sup>5</sup> The structures were checked using the software PLATON.<sup>6</sup> The absorption correction was performed using the SCALE3 ABSPACK multiscan method.<sup>7</sup> Visualization was done with the software Mercury.<sup>8</sup> NMR spectra were recorded on a Bruker AV400 NMR instrument. The spectrometer was externally referenced to  $\text{CFCl}_3$  for  $^{19}\text{F}$  NMR and to tetramethylsilane for  $^1\text{H}$  NMR spectra. For visualization and evaluation, the software MestReNova Version 14.3.2 was used.<sup>9</sup> The spectra were recorded inside a 4 mm FEP tube liner. The samples were transferred with nitrogen pressure from a reaction tube to the NMR FEP tube. The FEP tube was cooled down to  $-196^\circ\text{C}$ , evacuated, flame sealed, and at  $-60^\circ\text{C}$  tested for leakage. Immediately before the NMR measurement, the sealed FEP tube was

placed in a standard glass NMR tube filled with 0.2 mL of acetone d6 as an external reference and warmed to  $-60^{\circ}\text{C}$ . Quantum chemical calculations were performed using the Gaussian09 and Gaussian16 software packages,<sup>10</sup> and the GaussView 6 software package was used to visualize the calculated structures and mapped MEP surfaces.<sup>11</sup> Unless otherwise stated, all calculations were performed at the M06-2X/aug-cc-pVTZ level of theory.

**[SO<sub>2</sub>Me][SbF<sub>6</sub>]:** For the synthesis of [SO<sub>2</sub>Me][SbF<sub>6</sub>] first antimony pentafluoride (280 mg, 1.292 mmol, 1.0 eq.) was condensed into a reactor (FEP tube). Methyl fluoride (44 mg, 1.292 mmol, 1.0 eq) and SO<sub>2</sub> as solvent were added at  $-196^{\circ}\text{C}$ . The reaction was warmed up to  $-60^{\circ}\text{C}$  and mixed. The solvent was removed at  $-78^{\circ}\text{C}$  and [SO<sub>2</sub>Me][SbF<sub>6</sub>] was obtained.

**[FS(OMe)<sub>2</sub>][Sb<sub>2</sub>F<sub>11</sub>]:** To the [SO<sub>2</sub>Me][SbF<sub>6</sub>] salt Methyl fluoride (220 mg, 6.46 mmol, 5.0 eq) and SO<sub>2</sub> were added. The reaction mixture was warmed up to  $5^{\circ}\text{C}$  and mixed. The solvent was removed at  $-78^{\circ}\text{C}$  and [FS(OMe)<sub>2</sub>][Sb<sub>2</sub>F<sub>11</sub>] was obtained.

**[FS(OH)(OMe)][SbF<sub>6</sub>]** To the [SO<sub>2</sub>Me][SbF<sub>6</sub>] salt anhydrous HF was added as solvent and reagent. The reaction mixture was warmed up to  $5^{\circ}\text{C}$  and mixed. The solvent was removed at  $-78^{\circ}\text{C}$  and [FS(OMe)<sub>2</sub>][Sb<sub>2</sub>F<sub>11</sub>] was obtained.

## 6 References

- 1 L. Bayersdorfer, R. Minkwitz and J. Jander, Eine Infrarot-Tieftemperaturkette für die Vermessung temperaturempfindlicher Gase, Flüssigkeiten und Feststoffe, *Z. anorg. allg. Chem.*, 1972, **392**, 137–142.
- 2 Rigaku Oxford Diffraction, *CrysAlisPro Software System, Version 1.171.39.46e*, Rigaku Corporation, Oxford, UK, 2018.
- 3 G. M. Sheldrick, SHELXT - integrated space-group and crystal-structure determination, *Acta crystallogr., C Struct. chem., Foundations and advances*, 2015, **71**, 3–8.
- 4 G. M. Sheldrick, Crystal structure refinement with SHELXL, *Acta crystallographica. Section C, Structural chemistry*, 2015, **71**, 3–8.
- 5 L. J. Farrugia, WinGX suite for small-molecule single-crystal crystallography, *J. Appl. Crystallogr.*, 1999, **32**, 837–838.
- 6 A. L. Spek, Single-crystal structure validation with the program PLATON, *J. Appl. Crystallogr.*, 2003, **36**, 7–13.
- 7 *SCALE3 ABSPACK, An Oxford Diffraction Program*, Oxford Diffraction Ltd, UK, 2005.
- 8 C. F. Macrae, I. Sovago, S. J. Cottrell, P. T. A. Galek, P. McCabe, E. Pidcock, M. Platings, G. P. Shields, J. S. Stevens, M. Towler and P. A. Wood, Mercury 4.0 : from visualization to analysis, design and prediction, *J. Appl. Crystallogr.*, 2020, **53**, 226–235.
- 9 Mestrelab Research S.L., *MestReNova Version 14.0.0*, 2019.
- 10 M. J. Frisch, G. W. Trucks, H. B. Schlegel, G. E. Scuseria, M. A. Robb, J. R. Cheeseman, G. Scalmani, V. Barone, G. A. Petersson, H. Nakatsuji, X. Li, M. Caricato, A. V. Marenich, J. Bloino, B. G. Janesko, R. Gomperts, B. Mennucci, H. P. Hratchian, J. V. Ortiz, A. F. Izmaylov, J. L. Sonnenberg, Williams, F. Ding, F. Lipparini, F. Egidi, J. Goings, B. Peng, A. Petrone, T. Henderson, D. Ranasinghe, V. G. Zakrzewski, J. Gao, N. Rega, G. Zheng, W. Liang, M. Hada, M. Ehara, K. Toyota, R. Fukuda, J. Hasegawa, M. Ishida, T. Nakajima, Y. Honda, O. Kitao, H. Nakai, T. Vreven, K. Throssell, J. A. Montgomery Jr., J. E. Peralta, F. Ogliaro, M. J. Bearpark, J. J. Heyd, E. N. Brothers, K. N. Kudin, V. N. Staroverov, T. A. Keith, R. Kobayashi, J. Normand, K. Raghavachari, A. P. Rendell, J. C. Burant, S. S. Iyengar, J. Tomasi, M. Cossi, J. M. Millam, M. Klene, C. Adamo, R. Cammi, J. W. Ochterski, R. L. Martin, K. Morokuma, O. Farkas, J. B. Foresman and D. J. Fox, *Gaussian 16 Rev. C.01*, Gaussian, Wallingford, CT, 2016.
- 11 Roy Denningon, Todd A. Keith, John M. Millam, *GaussView Version 6*, 2019.